Upward electrical discharges from thunderstorms

PAUL R. KREHBIEL[1]*, JEREMY A. RIOUSSET[2]*, VICTOR P. PASKO[2], RONALD J. THOMAS[3], WILLIAM RISON[3], MARK A. STANLEY[4] AND HARALD E. EDENS[1]

[1]Physics Department, New Mexico Tech, Socorro, New Mexico 87801, USA
[2]CSSL Laboratory, Penn State University, University Park, Pennsylvania 16802, USA
[3]Electrical Engineering Department, New Mexico Tech, Socorro, New Mexico 87801, USA
[4]114 Mesa Verde Road, Jemez Springs, New Mexico 87025, USA
*e-mail: krehbiel@ibis.nmt.edu; riousset@psu.edu

Thunderstorms occasionally produce upward discharges, called blue jets and gigantic jets, that propagate out of the storm top towards or up to the ionosphere[1–4]. Whereas the various types of intracloud and cloud-to-ground lightning are reasonably well understood, the cause and nature of upward discharges remains a mystery. Here, we present a combination of observational and modelling results that indicate two principal ways in which upward discharges can be produced. The modelling indicates that blue jets occur as a result of electrical breakdown between the upper storm charge and the screening charge attracted to the cloud top; they are predicted to occur 5–10 s or less after a cloud-to-ground or intracloud discharge produces a sudden charge imbalance in the storm. An observation is presented of an upward discharge that supports this basic mechanism. In contrast, we find that gigantic jets begin as a normal intracloud discharge between dominant mid-level charge and a screening-depleted upper-level charge, that continues to propagate out of the top of the storm. Observational support for this mechanism comes from similarity with 'bolt-from-the-blue' discharges[5] and from data on the polarity of gigantic jets[6]. We conclude that upward discharges are analogous to cloud-to-ground lightning. Our explanation provides a unifying view of how lightning escapes from a thundercloud.

Classical, normally electrified thunderstorms have a dominant dipolar electrical structure consisting of mid-level negative and upper-level positive charges, augmented by lower positive charge and negative screening charge at the upper cloud boundary[7,8] (Fig. 1a). The storm charges and electric fields build up with time as a result of charging currents, believed to be precipitation driven[8], until a breakdown threshold is reached. At this point, bidirectional discharges occur[9,10], producing different lightning types depending on where the triggering occurs first.

Discharges that escape the storm are possible when the breakdown is triggered between adjacent unbalanced charge regions, such as occur in the lower and upper parts of storms[11–13]. Thus, breakdown triggered between the mid-level negative and lower positive charges usually escapes the storm downward to become a negative cloud-to-ground discharge[14] (Fig. 1b). The ability of the discharge to continue through the lower positive charge region is aided by the presence of an overall negative charge imbalance in the storm, which biases the storm potentials

negatively and imparts a strongly negative initial potential ('×' in Fig. 1c) to the downward-developing leader.

Normally electrified storms tend to develop an overall negative charge imbalance with time as a result of the negative screening charge flowing to the cloud top[15] (I_{sc} in Fig. 1a). The negative charge is intermittently lowered to ground by negative cloud-to-ground discharges, thereby helping charge the global atmospheric electric circuit[7]. Simple electrodynamic model calculations (see the Supplementary Information) show that the effect of a negative cloud-to-ground discharge is to suddenly change the storm's net charge from negative to positive. As a result, the cloud potential quickly shifts towards positive values (Fig. 1c) and the electric field is enhanced in the upper part of the storm[16] (Fig. 1b). Continued charging can lead to a discharge being triggered in the upper part of the storm within a few seconds (Fig. 1e,f), which would be expected to escape upward above the cloud top. The upward discharge would have the same polarity as the upper storm charge, namely positive for a normally electrified storm producing negative cloud-to-ground discharges. The triggering is suppressed if the screening charge is mixed into the upper storm charge, but if such mixing is weak or absent, upward discharges are predicted to occur commonly. The fact that jets are infrequent implies that mixing of the screening charge is normally strong in storms.

That an upper-level discharge, once triggered, would propagate upward above the cloud top is illustrated in Fig. 1d using results from a stochastic lightning simulation model[17]. The breakdown escapes upward because of the strong positive potential (~150 MV) in the upper part of the storm, which is imparted to the developing leader channel, coupled with the lack of a potential barrier for upward propagation[13] (Fig. 1f).

Figure 2 shows observations of an upward jet that agree with the basic mechanism described above. The observation was obtained with a three-dimensional very high-frequency (VHF) lightning mapping array[5] during the Severe Thunderstorm Electrification and Precipitation Study[18] (STEPS 2000), and was only recently discovered in the STEPS data. Until then no upward discharges had been seen or confirmed in the VHF mapping data. The jet occurred in a decaying storm system that had an inverted electrical structure[19] and was producing intracloud discharges between an upper layer of negative charge and positive charge below the
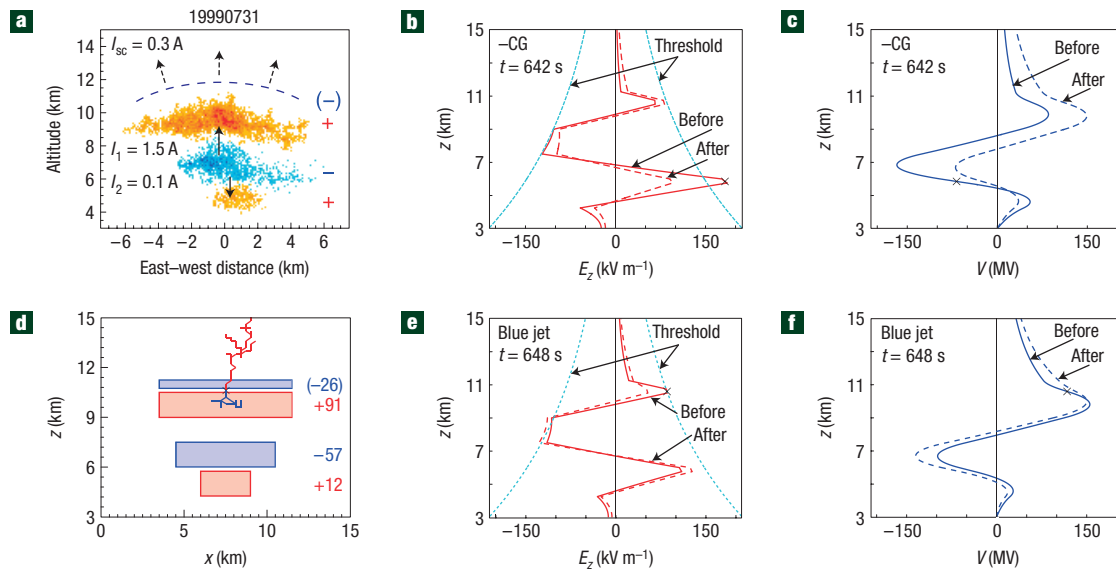
Figure 1 Basic scenario leading to blue jet formation. a, Lightning-inferred charge structure[14] and model-estimated charging currents in a normally electrified storm over Langmuir Laboratory on 31 July 1999, including the expected screening charge at the upper cloud boundary (dashed line). **b,c**, Vertical electric field (E_z) and potential (V) profiles before and after a negative cloud-to-ground (−CG) discharge, showing how the discharge increases V and E_z in the upper part of the storm, and the assumed breakdown threshold versus altitude. **d–f**, Simulated and predicted occurrence of an upward discharge 6 s after the negative cloud-to-ground discharge. × symbols denote E_z and V where each discharge is initiated.

negative. It was initiated midway between the upper negative charge and expected positive screening charge at the upper cloud boundary, 10 s after an intracloud discharge selectively removed positive charge from immediately below the initiation location (Fig. 2b–d). The jet lasted 120 ms and propagated 4 km upward in the first 60 ms ($v = 7 \times 10^4$ m s^{-1}) to 13.5 km altitude, 2 km above the radar-detected echo top (Fig. 2a). Its development was characteristic of an upward negative leader[5,20] that would have been visible above the cloud top. The polarity is confirmed by low-frequency electric field measurements of another, similar jet that occurred later in the same storm. Both discharges may have been similar to the optical 'gnome' observed later during STEPS[21].

The STEPS jet is well simulated using a cylindrical disc charge configuration in which the lower positive charge is reduced relative to the upper negative charge, and capped by a thin positive screening charge (Fig. 2e). Except for the polarities being reversed, the observations are fully consistent with the model of Fig. 1. The intracloud discharge locally unbalanced the storm charge in the vicinity of the initiation region and the upward breakdown occurred 10 s later, directly above the unbalanced region (Fig. 2b).

Other jets should have been detected by VHF mapping systems by now, but have not been. A possible explanation is that most blue-type jets are due to positive upward breakdown[22–24] that radiates weakly at VHF[5,12]. This inference agrees with optical observations of blue jets as occurring in negative cloud-to-ground-producing storms and being preceded by increases in negative cloud-to-ground activity in the storm[1,23,25]. The breakdown probably starts as a leader that transitions within a few kilometres of exiting the cloud top to a streamer-dominated form[22,26] that could continue to higher altitude. The downward negative breakdown that would accompany an upward positive blue jet (Fig. 1d) has not been identified in VHF mapping observations so far.

A second mechanism exists for producing an upward discharge that may explain the occurrence of gigantic jets[3,4]. Gigantic jets

extend to higher altitude than blue jets[1,2] and have a different appearance. The continuous positive leader-like propagation of optically observed blue jets[1,23,25] is contrasted with the impulsive rebrightening of gigantic jets[3], resembling negative leader processes. The estimated polarity of the gigantic jet observed by two of us[3] was an issue of considerable uncertainty and debate[22,24,27]. Subsequent further evidence indicated that the gigantic jet was produced by a normally electrified storm and was of negative polarity[6]. The rebrightening events were accompanied by low-frequency sferics corresponding to the upward transfer of negative charge, and the appearance of the gigantic jet in video was preceded 0.8 s earlier by an energetic positive narrow bipolar pulse characteristic of the onset of an upward negative intracloud flash[5,6,28]. The inferred negative polarity agrees with subsequent measurements of gigantic jet sferics[4].

The only way a negative gigantic jet could be produced by a normally electrified storm is that it originate in the mid-level negative storm charge. Evidence for how this can happen is provided by observations of 'bolt-from-the-blue' (BFB) lightning discharges (Fig. 3a). VHF mapping observations show that BFB discharges begin as regular, upward-developing intracloud flashes in normally electrified storms[5,20,28]. Instead of terminating in the upper positive charge, however, the breakdown continues horizontally out the upper side of the storm and turns downward to ground. Although the lightning channel outside the cloud seems to originate in the upper positive charge, the leader continues to be of negative polarity and the resulting cloud-to-ground stroke lowers negative charge to ground from the storm mid-level. The mapping observations show that BFB discharges are surprisingly common in normally electrified storms.

The fact that BFB discharges occur reveals a charge imbalance in which the upper positive charge is depleted in magnitude relative to the mid-level negative charge, most likely by mixing with upper screening charge. In exiting the cloud and turning towards ground, BFB discharges seem to be 'guided' by inferred positive screening
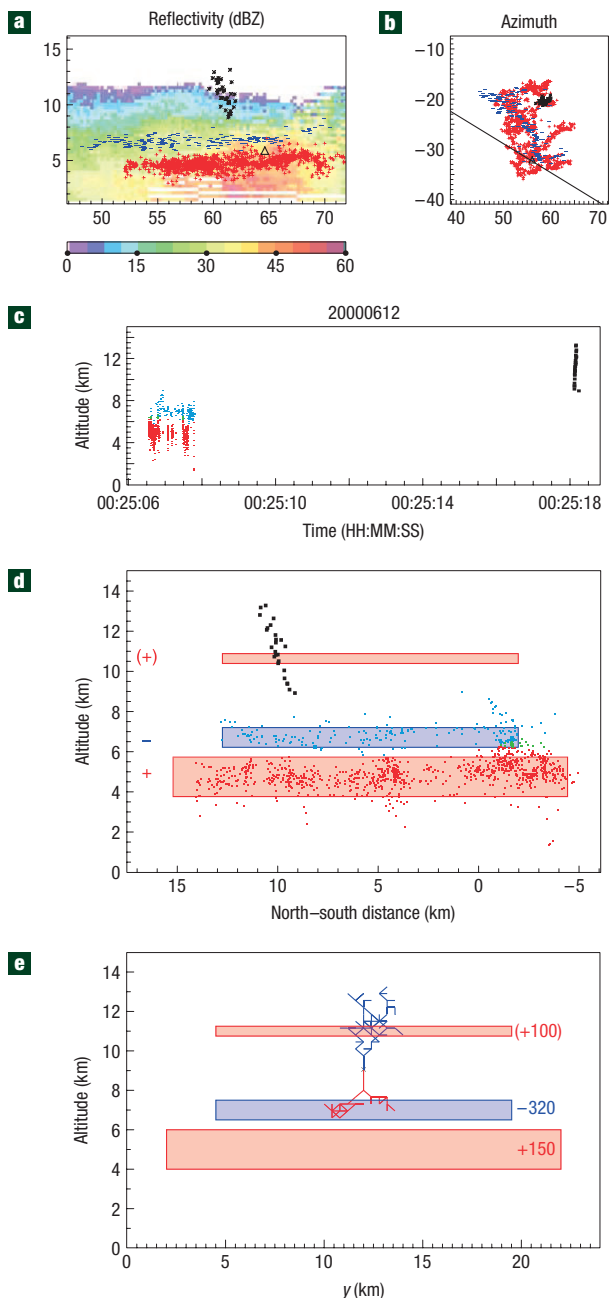
Figure 2 Upward negative jet from an inverted polarity storm on 12 June UTC **during STEPS 2000. a–d**, VHF mapping observations of the jet (filled black sources) and preceding intracloud discharge, projected onto the closest vertical radar scan through the storm (**a**; line in plan projection, **b**). The jet developed ~2 km above the echo top, beginning immediately above where the intracloud discharge locally removed positive charge from the lower storm level (**b**). Plan radar scans show that the radar top was essentially constant at ~11.5 km altitude above the flash and in the vicinity of the jet. **e**, Numerical simulation of the jet discharge.

charge attracted to the lateral cloud boundaries by the mid-level negative charge. This is supported by simulation experiments which find that substantial lateral charge is required to make the discharge turn downward to ground (Fig. 4e). In the absence of guiding charge, the preferred discharge mode is upward, as indicated by the negative gigantic jet simulation of Fig. 4f.
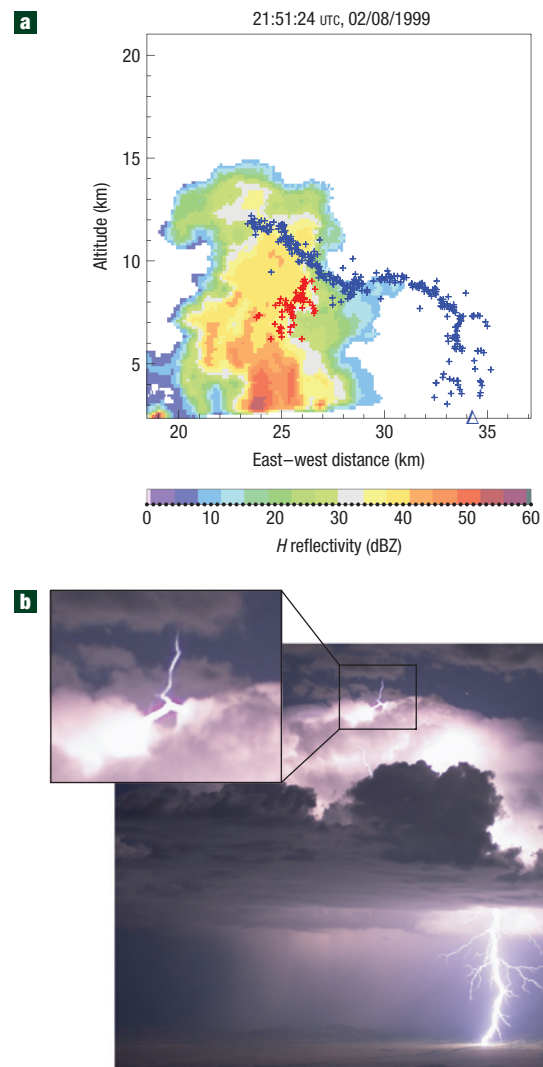

Figure 3 Two bolt-from-the-blue discharges. a, Lightning mapping observations of a negative BFB, superimposed on a vertical radar scan through the storm. The lightning began as an upward intracloud discharge between mid-level negative charge (red sources) and upper positive charge (blue sources), then exited the cloud and went to ground as a negative leader, well away from the storm. The 'triangle' denotes the negative cloud-to-ground strike point. **b**, A cloud-enshrouded BFB that started to develop upward above the storm top before branching horizontally back into the upper part of the storm and turning downward to ground, causing a negative cloud-to-ground discharge on the lower right.

Thus, upward discharges can occur as a result of an intracloud flash that encounters depleted upper positive charge and propagates on out of the top of the storm. That such a discharge can exit the storm top and start developing upward is indicated by a BFB photograph (Fig. 3b). Once initiated, the upward discharge can become 'gigantic' because it has as its source the main negative charge of the storm, capable of producing highly energetic discharges. Negative gigantic jets are thus the upward analogue of a downward cloud-to-ground discharge, with the role of the lower positive charge in triggering the discharge replaced by screening-depleted upper positive charge. In both cases, the lightning simulations show that continued propagation of the breakdown channels into the negative charge region maintains the channel
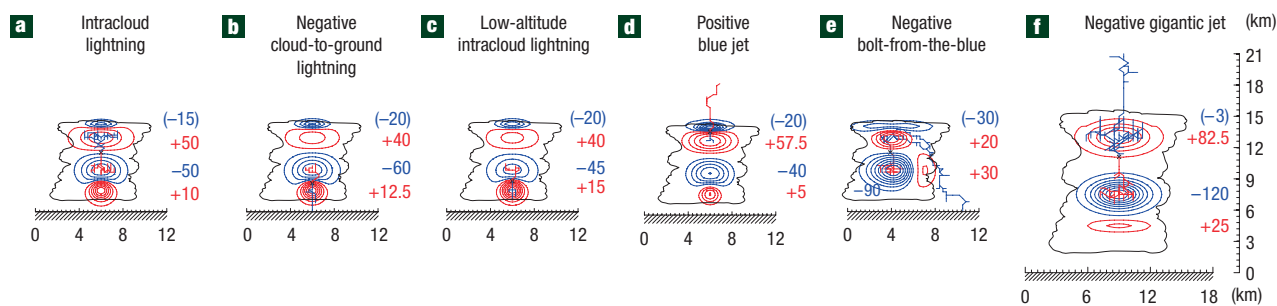
Figure 4 Simulated discharges illustrating the different known and postulated lightning types in a normally electrified storm. a–f, Blue and red contours and numbers indicate negative and positive charge regions and charge amounts (in C), respectively, each assumed to have a gaussian spatial distribution. A partially analogous set of discharges occurs or would be predicted to occur in storms having inverted electrical structures (see Supplementary Information, Fig. S5).

potential at a sufficiently high negative value for the opposite end of the discharge to propagate through the potential well[12] associated with the lower or depleted upper positive charge (for example, Fig. 1c).

At present, gigantic jets have been observed primarily at low latitudes and in storms extending to high altitudes (~15 km or more)[3,4]. This is possibly due to tropical clouds reaching high altitudes while remaining normally electrified[29]. Optical observations of blue jets also show them emanating at similarly high altitudes from clouds[1,25]. Other things being equal, blue jets would be more readily initiated in taller storms owing to the decrease in breakdown threshold with altitude (Fig. 1b,e).

Figure 4 summarizes the results of simulating the different discharge types in normally electrified storms. In all cases, the type results from a competition as to where breakdown is triggered first. Intracloud discharges usually win this competition because they occur between the two strongest charge regions during a storm's convective stages (Fig. 4a). Negative cloud-to-ground discharges (Fig. 4b,e) occur as descending precipitation generates lower positive charge[8] or as the storm accumulates net negative charge, and can go either directly to ground or indirectly as a BFB. Negative gigantic jets (Fig. 4f) provide an alternative way of relieving the mid-level negative charge, by discharging it to the upper atmosphere rather than to ground. Positive blue jets do the opposite, namely transport positive charge upward (Fig. 4d). Thus, positive blue jets contribute to the charging of the global electric circuit, whereas negative gigantic jets discharge the circuit. Mixing of the screening charge at the cloud top with the upper-level storm charge impedes the triggering of blue jets but encourages BFB and gigantic jet-type discharges. The degree of mixing therefore probably plays a fundamental role in the occurrence and frequency of jet phenomena. Strong mixing seems to be the norm, as demonstrated by the occurrence of BFB discharges. However, storms can get into the mode of producing blue jet-type breakdown[1,21]. The model calculations indicate that this can be the result of increased negative cloud-to-ground production that drives the net storm charge positive, or to decreased mixing in stratiform regions (see the Supplementary Information). In addition, the Fig. 2 observations show that blue jets can be instigated by intracloud discharges. Finally, blue-jet-type discharges are not necessarily confined to be lower-altitude cousins of gigantic jets, as both experience a similar, upwardly unconstrained potential environment once they escape the cloud top.

The results of this study illustrate both the symmetries and asymmetries of the possible discharge types in convective storms[30]. Whereas upward jets are symmetric analogues of downward cloud-to-ground discharges, they are substantially asymmetric in terms of their rate of occurrence. The discharge types are independent of polarity, giving rise for example to inverted intracloud and positive cloud-to-ground discharges in inverted polarity storms[18,19], as well as to the negative jet of Fig. 2. BFB discharges have not been observed in inverted storms, but it is possible that positive gigantic jets could be produced by such storms (see Supplementary Information, Fig. S5). Taken together, the upward breakdown types provide a set of scenarios that can be tested by further observations.

METHODS

LIGHTNING MAPPING AND RADAR OBSERVATIONS

The lightning observations of Figs 1a and 3a were obtained at Langmuir Laboratory using the New Mexico Tech Lightning Mapping Array[5]. The arrival times of impulsive radiation events in the 60–66 MHz VHF band were measured at six or more ground-based stations and were used to determine the development of individual lightning discharges in three-dimensional space and time. Differences in the radiation and propagation characteristics of negative and positive breakdown were used to determine the polarity of the lightning channels[5] (Figs 2a–d, 3a) and to infer the charge structure of an example storm[12,14,19] (Fig. 1a). Vertical radar scans from the National Center for Atmospheric Research S-Pol (10 cm) radar and New Mexico Tech (3 cm) dual-polarization radar provided the structure of the parent storm (Figs 2a and 3a, respectively).

ELECTRODYNAMIC STORM MODEL

The electrodynamic model (see the Supplementary Information) used the lightning polarity data of Fig. 1 as input to estimate the locations and extents of the storm charge regions. It represented the charge structure as a vertical sequence of axially aligned, uniformly charged cylindrical discs (see Supplementary Information, Fig. S1), for which the electric field and potential profiles were calculated along the axis. The storm charging currents were represented by two current sources, I_1 between the mid-level negative and upper positive storm charges, and I_2 between the negative and lower positive charges, the values of which were determined by running the model in time and matching the average flashing rates of intracloud and cloud-to-ground discharges to the observed flashing rates. An above-cloud, ohmic screening current I_{sc} was calculated by the model to simulate the formation of a screening charge at the upper cloud boundary. Lightning was assumed to occur when the on-axis electric field exceeded a specified altitude-dependent electric field threshold. Depending on the initiation location, intracloud, cloud-to-ground or upward jet discharges occurred and the charge content of the appropriate layers was decreased accordingly. The results revealed the role of the screening charge and mixing currents in the occurrence of upward discharges (see the Supplementary Information for further details).

LIGHTNING SIMULATION MODEL

The lightning model[17] uses a Lightning-Mapping-Array-inferred multilayered charge structure positioned above a perfectly conducting flat ground plane

(see main text and Fig. 1a). The thundercloud and lightning discharge are modelled in a three-dimensional cartesian domain using equidistant grids. The electric potential on the side and upper boundaries is calculated so that the contributions of all the charges within the simulation domain as well as their ground images are accounted for. These boundary conditions effectively represent 'open boundaries'. The potential at any point in the simulation domain is calculated with a successive overrelaxation method using the cloud charge structure and the boundary conditions described above. The development of bidirectional leaders starts when the cloud charges create an ambient field that exceeds a predefined threshold E_{init} anywhere in the simulation domain. Although controlled by different processes, the propagation thresholds of the positive and negative leaders are known to require nearly identical fields, which in the present study were assumed to be equal to the initiation threshold ($E_{init} = E_{th}^{\pm} = \pm 2.16 \, kV \, cm^{-1}$ at sea level)[17]. The initiation and propagation thresholds are assumed to scale with altitude z proportionally to the atmospheric neutral density $N(z)$. The simulated leader channel propagates iteratively; at each step, one and only one link is added at either the positive or negative end of the tree. Every point P of the discharge is scanned for its neighbours P'. Among the points P' which form with P a potential difference with corresponding electric field $E(P, P')$ such that $E(P, P') \geq E_{th}^{+}$ or $E(P, P') \leq E_{th}^{-}$, one is chosen to form the next stage of propagation according to the probability $p(P, P') = |E(P, P') - E_{th}^{\pm}| / \sum_{P, P'} |E(P, P') - E_{th}^{\pm}|$ (refs 17,22). After addition of the new segment, the potential is updated to ensure the overall neutrality of the equipotential channel[17]. The model therefore uses a fractal approach to introduce stochasticity in a self-consistent model of the lightning channel, which fully satisfies Kasemir's hypothesis of equipotentiality and overall neutrality of the discharge[9,11].

LIGHTNING PHOTOGRAPH

The BFB photograph of Fig. 3b was taken with a 38 s time exposure from Langmuir laboratory at 3,230 m altitude, 30 km distance from the storm, using an infrared-modified 6 megapixel Canon 300D digital single-lens reflex camera fitted with a Nikon 35 mm/2.0 lens set at f/5.6. The ISO-setting was 100, without noise reduction.

References

1. Wescott, E. M., Sentman, D., Osborne, D., Hampton, D. & Heavner, M. Preliminary results from the Sprites94 aircraft campaign: 2. Blue jets. *Geophys. Res. Lett.* **22**, 1209–1212 (1995).
2. Boeck, W. L. *et al.* Observations of lightning in the stratosphere. *J. Geophys. Res.* **100**, 1465–1475 (1995).
3. Pasko, V. P., Stanley, M. A., Matthews, J. D., Inan, U. S. & Wood, T. G. Electrical discharge from a thundercloud top to the lower ionosphere. *Nature* **416**, 152–154 (2002).
4. Su, H. T. *et al.* Gigantic jets between a thundercloud and the ionosphere. *Nature* **423**, 974–976 (2003).
5. Rison, W., Thomas, R. J., Krehbiel, P. R., Hamlin, T. & Harlin, J. A GPS-based three-dimensional lightning mapping system: Initial observations in central New Mexico. *Geophys. Res. Lett.* **26**, 3573–3576 (1999).
6. Mathews, J. D. *et al.* Electromagnetic signatures of the Puerto Rico blue jet and its parent thunderstorm. *Eos Trans. AGU* **83**, F91 (2002); Fall Meet. Suppl., Abstract A62D-02.
7. Krehbiel, P. R. *The Earth's Electrical Environment* 90–113 (Nat'l. Academy Press, Washington, 1986).
8. Williams, E. R. The tripolar structure of thunderstorms. *J. Geophys. Res.* **94**, 13151–13167 (1989).
9. Kasemir, H. W. A contribution to the electrostatic theory of a lightning discharge. *J. Geophys. Res.* **65**, 1873–1878 (1960).
10. Mazur, V. & Ruhnke, L. H. Common physical processes in natural and artificially triggered lightning. *J. Geophys. Res.* **98**, 12913–12930 (1993).
11. Mazur, V. & Ruhnke, L. H. Model of electric charges in thunderstorms and associated lightning. *J. Geophys. Res.* **103**, 23299–23308 (1998).
12. Coleman, L. M. *et al.* Effects of charge and electrostatic potential on lightning propagation. *J. Geophys. Res.* **108**, 4298 (2003).
13. Raizer, Y. P., Milikh, G. M. & Shneider, M. N. On the mechanism of blue jet formation and propagation. *Geophys. Res. Lett.* **33**, L23801 (2006).
14. Marshall, T. C. *et al.* Observed electric fields associated with lightning initiation. *Geophys. Res. Lett.* **32**, L03813 (2005).
15. Wilson, C. T. R. Investigations on lightning discharges and on the electric field of thunderstorms. *Phil. Trans. R. Soc. Lond. A* **221**, 73–115 (1921).
16. Wilson, C. T. R. A theory of thundercloud electricity. *Proc. R. Soc. Lond. A* **236**, 297–317 (1956).
17. Riousset, J. A., Pasko, V. P., Krehbiel, P. R., Thomas, R. J. & Rison, W. Three-dimensional fractal modeling of intracloud lightning discharge in a New Mexico thunderstorm and comparison with lightning mapping observations. *J. Geophys. Res.* **112**, D15203 (2007).
18. Lang, T. J. *et al.* The severe thunderstorm electrification and precipitation study. *Bull. Am. Meteorol. Soc.* **85**, 1107–1125 (2004).
19. Rust, W. D. *et al.* Inverted-polarity electrical structures in thunderstorms in the Severe Thunderstorm Electrification and Precipitation Study (STEPS). *Atmos. Res.* **76**, 247–271 (2005).
20. Behnke, S. A., Thomas, R. J., Krehbiel, P. R. & Rison, W. Initial leader velocities during intracloud lightning: Possible evidence for a runaway breakdown effect. *J. Geophys. Res.* **110**, D10207 (2005).
21. Lyons, W. A. *et al.* Upward electrical discharges from thunderstorm tops. *Bull. Am. Meteorol. Soc.* **84**, 445–454 (2003).
22. Pasko, V. P. & George, J. J. Three-dimensional modeling of blue jets and blue starters. *J. Geophys. Res.* **107**, 1458 (2002).
23. Wescott, E. M., Stenbaek-Nielsen, H. C., Huet, P., Heavner, M. J. & Moudry, D. R. New evidence for the brightness and ionization of blue jets and blue starters. *J. Geophys. Res.* **106**, 21549–21554 (2001).
24. Raizer, Y. P., Milikh, G. M. & Shneider, M. N. Leader–streamers nature of blue jets. *J. Atmos. Sol. Terr. Phys.* **69**, 925–938 (2007).
25. Wescott, E. M., Sentman, D. D., Heavner, M. J., Hampton, D. L. & Vaughan, O. H. Jr. Blue jets: Their relationship to lightning and very large hailfall, and their physical mechanisms for their production. *J. Atmos. Sol. Terr. Phys.* **60**, 713–724 (1998).
26. Petrov, N. I. & Petrova, G. N. Physical mechanisms for the development of lightning discharges between a thundercloud and the ionosphere. *Tech. Phys.* **44**, 472–475 (1999).
27. Sukhorukov, A. I. & Stubbe, P. Problems of blue jet theories. *J. Atmos. Sol. Terr. Phys.* **23**, 725–732 (1998).
28. Thomas, R. J. *et al.* Observations of VHF source powers radiated by lightning. *Geophys. Res. Lett.* **28**, 143–146 (2001).
29. Williams, E. R. *et al.* Lightning flashes conducive to the production and escape of gamma radiation to space. *J. Geophys. Res.* **111**, D16209 (2006).
30. Williams, E. R. Problems in lightning physics—the role of polarity asymmetry. *Plasma Sources Sci. Technol.* **15**, S91–S108 (2006).

Author contributions

P.R.K. drafted the manuscript and developed the electrodynamic model. J.A.R. carried out the lightning simulations, prepared the figures and drafted the methods section. J.A.R. and V.P.P. developed the lightning simulation model. W.R., R.J.T. and P.R.K. developed the Lightning Mapping Array, conducted the field programs and carried out the data analyses for the study. M.A.S. carried out low-frequency measurements and analyses. H.E.E. obtained the photograph of Fig. 3b. All authors contributed to discussion of the results and preparation of the manuscript.

Supplementary Information to 'Upward Electrical Discharges from Thunderstorms',

P. Krehbiel, J. Riousset, V. Pasko, R. Thomas, W. Rison, M. Stanley, H. Edens

Electrodynamic Model

In this section we describe the electrodynamic model used to simulate the electrical activity of a storm and present additional details of using the model to investigate the occurrence of upward discharges. The model represents the storm charges as a vertical sequence of axially aligned, uniformly-charged cylindrical disks (Fig. S1), for which the electric field and potential profiles are calculated on the axis of the disks (Fig. 1b,c,e,f)[31, 20]. The altitudes, thicknesses, and radii of the charge disks are determined from three-dimensional mapping observations of the lightning activity in the storm being studied. The lightning observations are obtained by the New Mexico Tech Lightning Mapping Array (LMA), which accurately locates the sources of impulsive VHF radiation events in three spatial dimensions and time[32]. By analyzing the structure and development of individual lightning flashes, one is able to determine the location and polarity of the charge regions being penetrated by the discharge channels[33, 34, 19]. From an analysis of sequences of flashes, a picture is obtained of the charge structure of the storm involved in the lightning (Fig. 1a)[14, 19].

Figure S1. Cylindrical charge configuration of the electrodynamic model for a normally electrified storm, showing positive (red) and negative (blue) charge regions, and storm currents.

For a normally-electrified storm, two currents are used to simulate the storm charging: a main current I_1 between the mid-level negative (N) and upper positive (P) charge regions, and a second current I_2 between the N and lower positive (LP) regions. An above-cloud, ohmic 'screening' current I_{sc} is calculated by the model to account for charge attracted to the cloud top from the conducting clear air above the storm. The current causes a layer of negative charge to form at the upper cloud boundary[35], called the screening charge, that reduces the electric field above the cloud. The screening charge is represented by the uppermost disk in the model. The parameters of the charge regions used in this study are listed in Supplementary Table 1 and correspond to a July 31, 1999 storm[14] over Langmuir Laboratory in central New Mexico (3.2 km altitude above mean sea level).

Given the storm's basic charge structure, the charging currents I_1 and I_2 are estimated by running the model in time and adjusting the currents to reproduce the observed average lightning rates[31]. Lightning is assumed to occur when the on-axis electric field exceeds a specified threshold value versus altitude. The threshold relation used in this study is $E_{\text{thresh}} = E_0\, e^{-z/z_0}$, where $E_0 = 302$ kV m^{-1} and the scale height $z_0 = 8.4$ km. The $E_{\text{thresh}}(z)$ values provide a good empirical estimate of the electric field at which lightning is initiated during in-cloud balloon-borne soundings[36, 14, 37], with E_0 being 40% higher than the breakeven electric field $E_{be} = 216$ kV m^{-1} for energetic electron avalanches at sea level[38]. Lightning initiated between the N and P charge regions results in a normal intracloud (IC) discharge, while lightning initiated between the N and lower
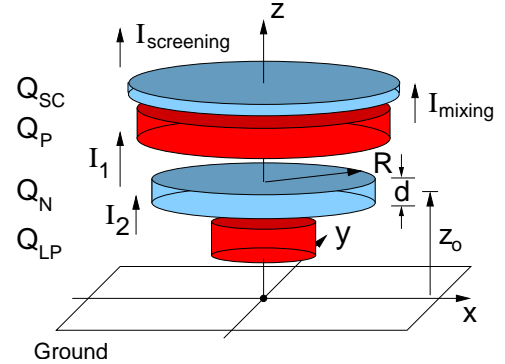
positive regions results in a negative cloud-to-ground ($-$CG) discharge. IC discharges were nominally assumed to reduce the pre-flash storm charges by 50% of the lesser of charges Q_N and Q_P. CG discharges reduced Q_N and Q_{LP} by 50% each (assuming $|Q_{LP}| < |Q_N|$), with the difference being the charge lowered to ground. The resulting changes in Q_N and Q_P were typically 30-40 C, comparable to values determined from lightning electric field change measurements[39, 40, 41].

During the active stage of the July 31, 1999 storm, the storm produced 9 negative CG flashes and 30 IC flashes over a 14 min. time interval[31]. These average flashing rates are reproduced by the model for an upward charging current $I_1 = 1.5$ A between the main dipolar (N, P) charge regions and a downward current $I_2 = -0.1$ A into the lower positive charge (Fig. 1a). The average screening current to the cloud top was $I_{sc} = 0.31$ A. To match the relative IC and CG rates, the criteria for CG discharges needed to be more stringent than that obtained from the threshold relation itself; this was accomplished by requiring the electric field E to exceed the breakdown threshold over a nominal vertical distance of 500 m before a CG flash was initiated (Fig. 1b).

Fig. S2 shows the variation of the storm charges and currents with time. During the first 400 s, I_1 and I_2 have the values that reproduce the average flashing rates. The storm behaves as a classic relaxation oscillator wherein the charging currents produce linear charge increases that are periodically relaxed by IC discharges and, less often, by CG discharges. The electric field and screening current above the cloud are predominantly upward-directed, corresponding to the downward transport of negative screening charge to the cloud top. This steadily drives the overall storm charge toward negative values until a $-$CG occurs (Fig. S2b). The sudden removal of negative charge causes the overall storm charge to revert to a positive value, at which point the cycle repeats. Actual storms are not as deterministic as the simple model, but exhibit similar basic behavior.

An important result of the model calculations has been that, when the cloud-top screening current and charge are accounted for, discharges are predicted to be initiated regularly between the upper positive (P) and negative screening (SC) charges in the uppermost part of the storm[31, 42]. Due to the imbalance in the magnitudes of the two charges, such breakdown would be expected to escape the cloud upward. The fact that upward jets do not occur in most storms leads to the conclusion that the screening charge is normally dissipated in some way, most likely by being mixed into the upper positive charge. Because atmospheric ions quickly become immobilized on cloud particles inside the storm[43], such mixing would occur by convective overturning and turbulent processes or by a non-linear field-limiting process[44, 45], rather than by steady ohmic conduction*. The degree of mixing required to suppress the upper level breakdown is relatively strong; for the simulations of this study (including those of Fig. S2) the mixing was such that a non-replenished screening charge would be relaxed away exponentially with a time constant $\tau_{mix} \simeq 60$ s.

For a given mixing rate, the model simulations indicate that upper level discharges can occur if the charging currents in the storm are increased. This is seen after $t = 400$ s in Fig. S2. At that time both currents are doubled in magnitude, to $I_1 = 3.0$ A and $I_2 = -0.2$ A. This has the immediate effect of doubling the IC and CG flashing rates. In addition, over the next few minutes it also causes the net storm charge to drift toward an average positive value (Fig. S2b). The shift in net charge increases the vertical electric field in the upper part of the storm and leads to two upper-level discharges being triggered in the simulation. Electric field and potential profiles for the first of the indicated discharges, at $t = 648$ s, have been presented in Fig. 1. The discharges would

---

*Ion attachment causes electrical conduction currents to be negigibly small in clouds[46]; the model thus assumes the electrical conductivity to be zero inside the storm.
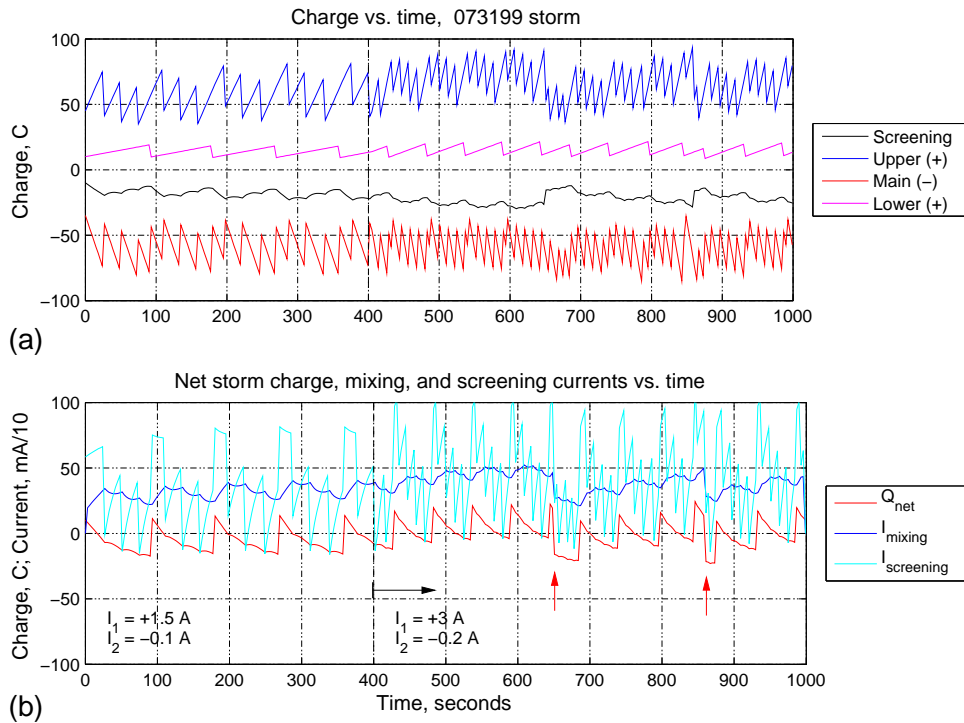
2

Figure S2: Model-calculated temporal variation of the storm charges and currents, showing the behavior that reproduces the average CG and IC flashing rates (t = 0 to 400 s) and the effect of doubling the charging currents (starting at t = 400 s). During the initial time interval, the screening current drives the overall storm charge Q_{net} toward negative values, while $-$CG discharges suddenly change the net charge to positive values (red line, panel b). The effect of increasing the charging current is to double the IC and CG flashing rates and to cause Q_{net} to develop a positive offset. The latter leads to the occurrence of upward discharges (red arrows), which cause changes in the screening charge, net charge, and mixing current (black line, panel a; red and blue lines, panel b).

transport positive charge upward (Fig. 1d) and are consistent with being of the blue jet variety. They are predicted to occur shortly after a CG discharge removes negative charge from the storm, which maximizes the storm's positive charge (Fig. S2b) and increases the vertical electric field in the upper part of the cloud (Fig. 1b).

The primary impetus for the onset of upper level discharges in the above simulation is the increased rate of occurrence of $-$CG discharges. This is indicated by the simulation of Fig. S3. Instead of increasing both charging currents, I_1 remains constant at 1.5 A and only the lower positive charging current I_2 is increased, in this case by a factor of three, to $I_2 = -0.3$ A. This increases the $-$CG rate correspondingly while the IC rate remains essentially as before. As in Fig. S2, the net storm charge drifts to an average positive value and upper-level discharges are indicated to start several minutes later, again shortly after $-$CG discharges. The positive charge build-up results from the increased rate at which the CGs remove negative charge from the storm.

The above results indicate that BJs can occur during episodes of enhanced $-$CG activity or increased overall lightning rates. The simulation of Fig. S4 illustrates how reduced mixing of the screening charge can also result in BJs, at normal charging rates. In this simulation no mixing is assumed and the charging rates are left at their original value throughout the full time interval. Upward discharges are predicted to occur frequently, nearly as often as the $-$CG flashes, and without the storm needing to develop average net positive charge. Both features result from the
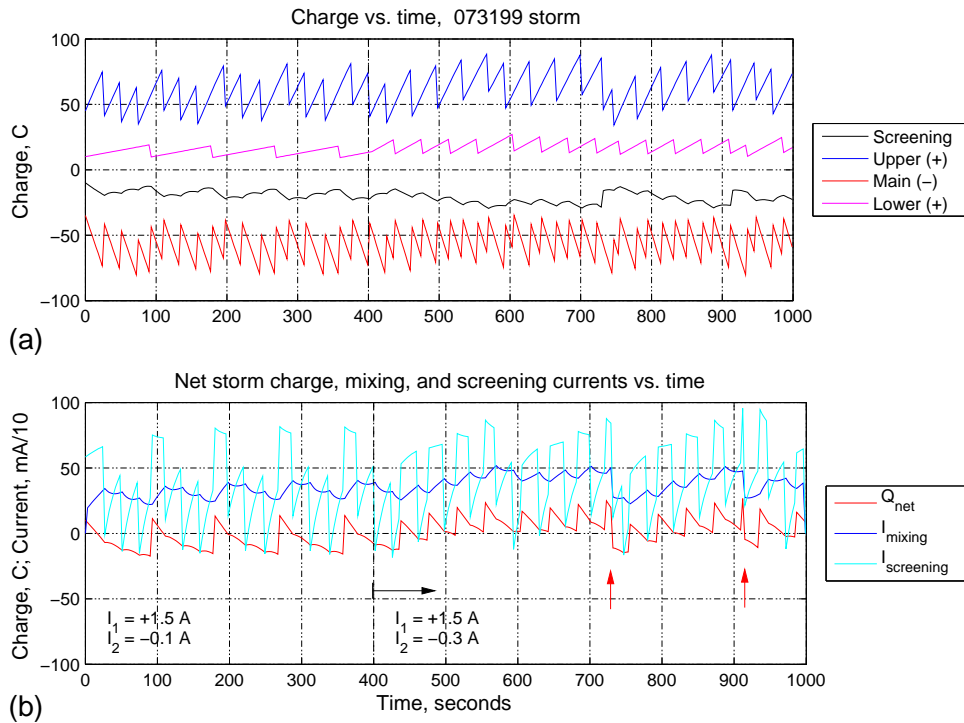
3

Figure S3: Same as Fig. S2, except that only the lower positive charging current I_2 is increased, showing that the drift to net positive storm charge and the occurrence of upward discharges results from the increase in the $-$CG flashing rate.

electric field in the upper part of the cloud not being reduced by mixing. The upward discharges continue to be instigated by $-$CG flashes, but the increased favorability for such breakdown is reflected in some upward discharges occurring after an intervening IC flash and also during the initiating CG (Fig. S4b). The STEPS jet of Fig. 2 occurred in a relatively stratiform part of the storm and its occurrence may have benefited from reduced mixing.

In all simulations, the screening charge plays the same role in enhancing the electric field and triggering blue jet discharges as the lower positive charge plays in triggering $-$CG discharges.[†] While $-$CG discharges occur on their own, BJs require a charge-imbalancing precursor discharge (such as a $-$CG) to make their triggering possible. In addition, rather than being triggered immediately during the precursor, as in Wilson's original suggestion[16], the breakdown is often delayed 5 to 10 s or so after the initiating flash. In the simulations, the delay is manifested by the electric field not immediately exceeding the breakdown threshold after the CG, so that additional charging is required for the threshold to be reached. The basic reason for the time delay is more subtle than this, however, and has to do with a) the buildup of conditions favorable to blue jets occurring gradually with time, and b) the fact that, after each CG, the BJs have to compete with normal IC flashes to be the next discharge in the storm[‡]. That upward discharges compete with intracloud

[†]Rather than being initiated in the clear air above the cloud boundary and requiring an unrealistically strong electric field above the cloud for the discharge to propagate upward, as in the study by Sukhorukov *et al.*[47], the above-cloud field is reduced by the screening charge (Fig. 1e) and the upward discharges are triggered in the cloud interior. The breakdown develops upward primarily by virtue of its channels being maintained at the high electric potential of the upper part of the storm (Fig. 1f). In addition, the upward breakdown is not restricted to be of negative polarity.

[‡]In particular, after each CG discharge the possibility exists of the next discharge being an IC flash between the N and P charge regions or upper-level breakdown between the P and negative screening charge (e.g., Fig. 1b). IC
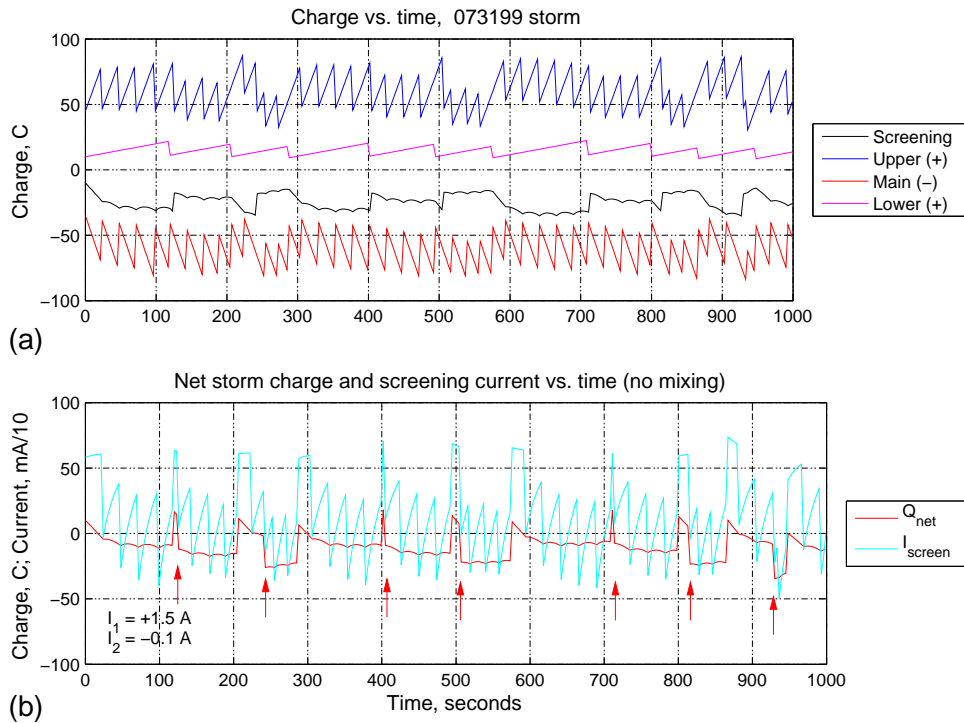
Figure S4: Same as Fig. S2, except that the screening charge is not mixed into the upper positive charge, showing the occurrence of a number of upward discharges are predicted to occur in the absence of such mixing. The charging currents remained constant throughout the full time interval. The storm does not need to develop a net positive charge for the upward discharges to be triggered, and upward discharges are predicted to occur almost as often as $-$CG discharges.

flashes, and are usually preempted by the ICs, is an important point seen both in the electrodynamic calculations and in the lightning simulations that has not been fully considered in previous studies[22, 48, 13]. Finally, BJs are not precluded from being triggered immediately during the precursor discharge. This can happen either by chance or by the precursor removing a large fraction of the mid-level charge.

Assuming that upward discharges reduce the upper positive and screening charges by 50% each, analogous to CG discharges, the net upward charge transfer is typically +40-45 C, somewhat larger in magnitude than the $-$CG charge amounts.

Supporting Discussion

The electrodynamic simulations suggest that blue jet discharges occur in parts of a storm where mixing of the screening charge is reduced, and/or during episodes of enhanced CG activity in a storm. Both scenarios are consistent with observational data on BJs, as discussed in the main part of the paper and in more detail below. For storms having enhanced $-$CG activity, the increased rate at which negative charge is lowered to ground causes the storm to develop an average net positive

---

flashes almost always win this competition by virtue of the N and P regions being charged actively by the main storm current, I_1. (By contrast, the screening charge is derived from the passive screening current.) As conditions following each CG flash become increasingly favorable for an upward discharge, the way the discharge finally happens is by getting close enough to being triggered to win the competition during the post-CG charging interval, rather than waiting to be produced immediately during a later CG. These features of the simulations are supported by the observational result that BJs do not occur simultaneously with other discharges in the storm.

charge, thereby increasing the clear-air flow of negative screening charge to the cloud boundary. The equilibrium average positive charge would be such that the increased negative screening influx balances the average outflux due to the $-$CG discharges. Because of the exponential increase of clear-air electrical conductivity with altitude, most of the negative charge flow is to the upper cloud boundary. Blue jets provide an alternate way of balancing the negative CG outflux (equivalently, a positive charge influx), by transporting positive charge out of the upper cloud boundary. Similarly, negative blue jets would tend to be produced by inverted polarity storms following episodes of enhanced $+$CG activity.

As noted in a number of studies, storms have periods of increased cloud-to-ground lightning, both negative[49, 50] and positive[34, 51]. In this and previous studies[52], model calculations indicate that the CG rate is controlled primarily by the amount of lower storm charge. For example, in Figs. S2 through S4, $-$CG discharges were initiated whenever the lower positive charge increased to $\sim$15-20 C, more or less independent of the net storm charge and of the intracloud activity. This indicates that the rate at which $-$CGs occur depends primarily on the strength of the lower positive charging current I_2 and leads to the inference or prediction that blue jets are favored in a storm when the lower positive charging increases. Such a situation would be expected when hail or graupel is being produced by a storm, due to reverse-polarity (positive) charging of hail during hail-ice crystal collisions[8, 50, 52].

The prediction that blue jets would be preceded by CG discharges is consistent with the limited observational evidence of storms that produce such discharges. The studies by Wescott *et al.*[53, 25] found a statistical increase in the cumulative number of $-$CG discharges a few seconds prior to the occurrences of the blue jets and blue starters, followed by a decrease in the number of $-$CGs for a few seconds after the occurrences. The effect was most pronounced for blue jets but was also seen for blue starters. 10 out of 27 temporally isolated blue jets were found to have occurred within 1 s after a National Lightning Detection Network (NLDN)-indicated $-$CG discharge within 15 km of the jet[25]. An additional 11 $-$CGs occurred 1 to 5 s prior to the jet occurrences. Analogous results were obtained for blue starters[53]. The reduction or apparent 'lull' in the $-$CG activity following the jets and starters would have reflected the time before the next $-$CG occurred. The starters and jets did not appear to be associated with particular lightning discharges, as most starters were found to 'arise out of the anvil during a quiet (lightning) interval.' However, the occurrence of $-$CG flashes prior to the upward discharges was considered possibly to be a 'factor in creating the electric field configuration leading to the initiation of (the) blue starters and jets.' The blue starters were found to be loosely concentrated near the centroid of the overall $-$CG activity, and also somewhat near the location of reported large hail.§ In a later study[23], a single blue jet was observed to occur within 4 s of a $-$CG discharge 14 km from the estimated location of the jet.

The recent report of a gigantic discharge over northeastern Mexico[55], published while this paper was in review, shows a possible similar correlation with CG activity. The discharge occurred following a 4-minute increase in the NLDN-detected $+$CG rate in one of two storms that could have been the source of the event. The increase culminated in a 20-s 'jump' in the $+$CG rate, to

---

§We note that the jet-producing Arkansas storm system was similar to the June 11 STEPS storm[54] that produced the negative jet of Fig. 2, in that both produced severe winds and hail and developed above 15 km altitude in their convective cores. The STEPS storm and other storms like it[19, 51, 56] generally consist of a combination of inverted- and normal-polarity electrical structures, and produce both positive and negative CGs. The Arkansas storm may have been partially or substantially inverted as well, raising the question whether some of the Arkansas jets were like the STEPS jet and were negative rather than positive polarity.
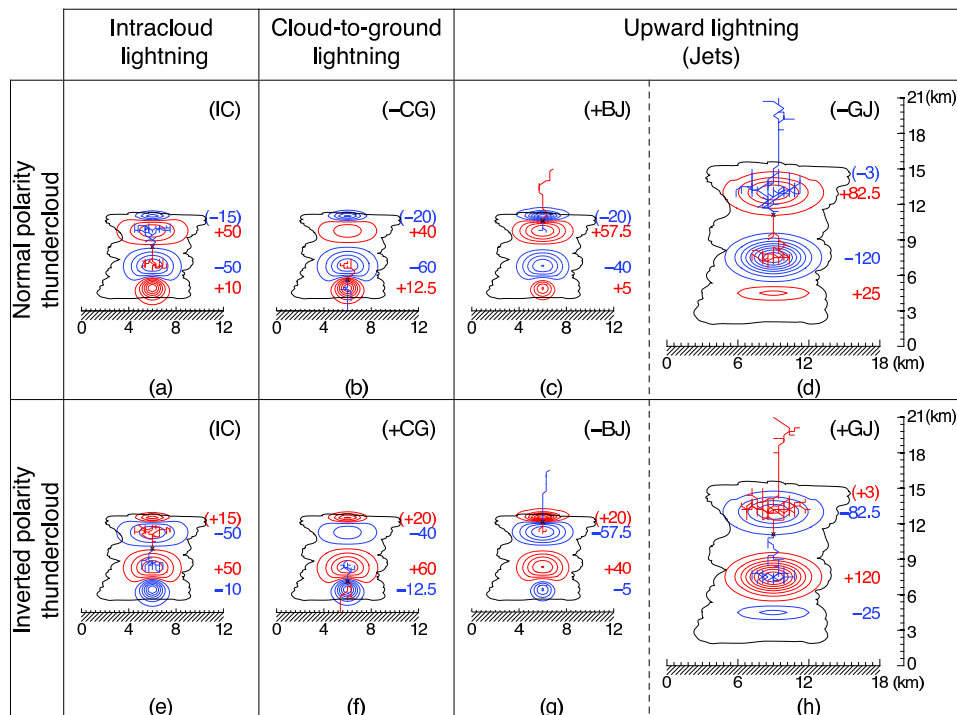
6

Figure S5: Illustrative lightning simulations for normal- and inverted-polarity storms, showing the four possible types of upward discharges, classified by initiation mechanism (blue jet and gigantic jet) and upward polarity (+ and −). Also shown for reference are the common forms of IC and CG flashes in normal and inverted storms. Blue jets will tend to be initiated by a precursor discharge (either CG or IC) that causes a charge imbalance in the storm.

one flash every 5 s, prior to the discharge's occurrence. The upward discharge was thought to be of negative polarity and to have originated in the upper negative charge of an inverted-polarity storm. If so it would have been a large blue jet-type discharge similar in its initiation mechanism to the STEPS jet of Fig. 2, but in a storm with a higher cloud top (∼14 km above mean sea level).

We have classified upward discharges into two basic categories or types: 'blue' jets (BJs) and 'gigantic' jets (GJs). Heretofore, the two types have been distinguished primarily in terms of their maximum altitudes, and possibly their polarities, with blue jets (including blue starters) developing up to lower altitudes than gigantic jets, and appearing to transport positive charge upward, while gigantic jets transport negative charge upward. If it is assumed that the two types are produced by normally electrified storms, as the observational information has indicated, the present study indicates that the distinguishing characteristic between them is where they are initiated relative to the storm charges. The resulting breakdown scenarios give rise to positive blue jets (+BJs) and negative gigantic jets (−GJs).

In addition to the above, the observations of Fig. 2 show that negative upward jets can be produced by inverted polarity storms. We identify this as a negative blue jet (−BJ) based on where it was initiated relative to the storm charges. By extension, the inverted-storm analog of a −GJ would be a +GJ, with each polarity of GJ having as its source the main or mid-level charge of the storm. The four possible types of upward discharges are summarized in Fig. S5.

****

7

Table S1: Heights and extents of charge regions for cylindrical disk model; storm of July 31, 1999 over Langmuir Laboratory (3 km MSL), and average charge values corresponding to the observed lightning rates.

Charge Layer	Altitude (km AGL[a])	Altitude (km MSL[b])	Depth (km)	Radius (km)	Avg. Charge (C)
Screening (SC)	8.00	11.00	0.5	4.0	−20
Upper Positive (P)	6.75	9.75	1.5	4.0	+60
Mid-level Negative (N)	3.75	6.75	1.5	3.0	−58
Lower Positive (LP)	2.00	5.00	1.5	1.5	+13

[a] AGL, above ground level;   [b] MSL, above mean sea level

References

1. Wescott, E. M., Sentman, D., Osborne, D., Hampton, D. & Heavner, M. Preliminary results from the Sprites94 aircraft campaign: 2. Blue jets. *Geophys. Res. Lett.* **22**(10), 1209–1212 (1995).

2. Boeck, W. L. *et al.* Observations of lightning in the stratosphere. *J. Geophys. Res.* **100**, 1465–1475 (1995).

3. Pasko, V. P., Stanley, M. A., Matthews, J. D., Inan, U. S. & Wood, T. G. Electrical discharge from a thundercloud top to the lower ionosphere. *Nature* **416**, 152–154 (2002).

4. Su, H. T. *et al.* Gigantic jets between a thundercloud and the ionosphere. *Nature* **423**, 974–976 (2003).

5. Rison, W., Thomas, R. J., Krehbiel, P. R., Hamlin, T. & Harlin, J. A GPS-based three-dimensional lightning mapping system: Initial observations in central New Mexico. *Geophys. Res. Lett.* **26**(23), 3573–3576 (1999).

6. Mathews, J. D., Stanley, M. A., Pasko, V. P., Wood, T. G., Inan, U. S., Heavner, M. J. & Cummer, S. A. Electromagnetic signatures of the Puerto Rico blue jet and its parent thunderstorm. *Eos Trans. AGU* **83**(47) (2002). Fall Meet. Suppl., Abstract A62D-02.

7. Krehbiel, P. R. *The electrical structure of thunderstorms*, in The Earth's Electrical Environment, 90–113, Nat'l. Academy Press, Washington, D.C., 1986.

8. Williams, E. R. The tripolar structure of thunderstorms. *J. Geophys. Res.* **94**(D11), 13151–13167 (1989).

9. Kasemir, H. W. A contribution to the electrostatic theory of a lightning discharge. *J. Geophys. Res.* **65**(7), 1873–1878 (1960).

10. Mazur, V. & Ruhnke, L. H. Common physical processes in natural and artificially triggered lightning. *J. Geophys. Res.* **94**, 12913–12930 (1993).

11. Mazur, V. & Ruhnke, L. H. Model of electric charges in thunderstorms and associated lightning. *J. Geophys. Res.* **103**(D18), 23299–23308 (1998).

12. Coleman, L. M. *et al.* Effects of charge and electrostatic potential on lightning propagation. *J. Geophys. Res.* **108**(D9), 4298 (2003).

13. Raizer, Y. P., Milikh, G. M. & Shneider, M. N. On the mechanism of blue jet formation and propagation. *Geophys. Res. Lett.* **33**(23), L23801 (2006).

14. Marshall, T. C. *et al.* Observed electric fields associated with lightning initiation. *Geophys. Res. Lett.* **32**(3), L03813 (2005).

15. Wilson, C. T. R. Investigations on lightning discharges and on the electric field of thunderstorms. *Phil. Trans. Roy. Soc. Lond., A* **221**, 73–115 (1921).

16. Wilson, C. T. R. A theory of thundercloud electricity. *Proc. Roy. Soc. Lond., A* **236**, 297-317 (1956).

17. Riousset, J. A., Pasko, V. P., Krehbiel, P. R., Thomas, R. J. & Rison, W. Three-dimensional fractal modeling of intracloud lightning discharge in a New Mexico thunderstorm and comparison with lightning mapping observations. *J. Geophys. Res.* **112**(D15203) (2007).

18. Lang, T. J. *et al.* The severe thunderstorm electrification and precipitation study. *Bull. Am. Meteorol. Soc.* **85**(8), 1107–1125 (2004).

19. Rust, W. D. *et al.* Inverted-polarity electrical structures in thunderstorms in the Severe Thunderstorm Electrification and Precipitation Study (STEPS). *Atmos. Res.* **76**(1–4), 247–271 (2005).

20. Behnke, S. A., Thomas, R. J., Krehbiel, P. R. & Rison, W. Initial leader velocities during intracloud lightning: Possible evidence for a runaway breakdown effect. *J. Geophys. Res.* **110**, D10207 (2005).

21. Lyons, W. A. *et al.* Upward electrical discharges from thunderstorm tops. *Bull. Am. Meteorol. Soc.* **84**(4), 445–454 (2003).

22. Pasko, V. P. & George, J. J. Three-dimensional modeling of blue jets and blue starters. *J. Geophys. Res.* **107**(A12), 1458 (2002).

23. Wescott, E. M., Stenbaek-Nielsen, H. C., Huet, P., Heavner, M. J. & Moudry, D. R. New evidence for the brightness and ionization of blue jets and blue starters. *J. Geophys. Res.* **106**(A10), 21549–21554 (2001).

24. Raizer, Y. P., Milikh, G. M. & Shneider, M. N. Leader–streamers nature of blue jets. *J. Atmos. Solar-Terr. Phys.* **69**(8), 925–938 (2007).

25. Wescott, E. M., Sentman, D. D., Heavner, M. J., Hampton, D. L. & Vaughan Jr., O. H. Blue jets: their relationship to lightning and very large hailfall, and their physical mechanisms for their production. *J. Atmos. Solar Terr. Phys.* **60**, 713–724 (1998).

26. Petrov, N. I. & Petrova, G. N. Physical mechanisms for the development of lightning discharges between a thundercloud and the ionosphere. *Tech. Phys.* **44**, 472–475 (1999).

27. Sukhorukov, A. I. & Stubbe, P. Problems of blue jet theories. *J. Atmos. Solar Terr. Phys.* **23**(13), 725–732 (1998).

28. Thomas, R. J. *et al.* Observations of VHF source powers radiated by lightning. *Geophys. Res. Lett.* **28**(1), 143–146 (2001).

29. Williams, E. R. *et al.* Lightning flashes conducive to the production and escape of gamma radiation to space. *J. Geophys. Res.* **111**, D16209 (2006).

30. Williams, E. R. Problems in lightning physics - the role of polarity asymmetry. *Plasma Sources Sci.& Tech.* **15(2)**, S91-S108 (2006).

31. Krehbiel, P. R. *et al.* Thunderstorm charge studies using a simple cylindrical charge model, electric field measurements, and lightning mapping observations. *Eos Trans. AGU* **85**(47) (2004). Fall Meet. Suppl., Abstract AE23A-0843.

32. Thomas, R. J. *et al.* Accuracy of the Lightning Mapping Array. *J. Geophys. Res.* **109**, D14207 (2004).

33. Thomas, R. J. *et al.* New Mexico thunderstorms observed by the lightning mapping array, an overview of one season. *Eos Trans. AGU* **83**(47) (2002). Fall Meet. Suppl., Abstract A71B-0097.

34. Hamlin, T. D. The New Mexico Tech Lightning Mapping Array. Ph. D. Dissertation, New Mexico Inst. Mining & Tech., available at http://hdl.handle.net/10136/40, 164 pp., (2004).

35. Brown, K. A., Krehbiel, P. R., Moore, C. B. & Sargent, G. N. Electrical screening layers around electrified clouds. *J. Geophys. Res.* **76**, 2825-2835 (1971).

36. Marshall, T. C., McCarthy, M. P. & Rust, W. D. Electric field magnitudes and lightning initiation in thunderstorms. *J. Geophys. Res.* **100**, 7097-7103 (1995).

37. Stolzenburg, M. *et al.* Electric field values observed near lightning flash initiations. *Geophys. Res. Letts.* **34**, L04804, doi:10.1029/2006GL028777, (2007).

38. Gurevich, A. V. & Zybin, K. P. Runaway breakdown and electric discharges in thunderstorms. *Phys. Uspekhi* **44**, 1119-1140 (2001).

39. Krehbiel, P. R., Brook, M. & McCrory, R. A. An analysis of the charge structure of lightning discharges to ground. *J. Geophys. Res.* **84**, 2432-2456 (1979).

40. Krehbiel, P. R. An analysis of the electric field change produced by lightning. Ph. D. Dissertation, Univ. Manchester Inst. Sci. & Tech., available at http://hdl.handle.net/10136/92, 459 pp. (1981).

41. Uman, M. A. *The Lightning Discharge.* Acad. Press, 377 pp. (1987).

42. Krehbiel, P. R. On the initiation of upward lightning discharges above thunderstorms. *Eos Trans. AGU* **86**(18) (2005). Jt. Assem. Suppl., Abstract AE11A-05.

43. Pruppacher, H. R. & J. D. Klett *Microphysics of Clouds and Precipitation.* D. Reidel, Dordrecht, (1978).

44. Eack, K. B., Beasley, W. H., Rust, W. D., Marshall, T. C. & Stolzenberg, M. Initial results from simultaneous observation of X rays and electric fields in a thunderstorm. *J. Geophys. Res.* **101**, 29637-29640 (1996).

45. Dwyer, J. R. A fundamental limit on electric fields in air. *Geophys. Res. Letts.* **30**, 2055 doi:10.1029/2003GL017781 (2003).

46. Rust, W. D. & Moore, C. B. Electrical conditions near the bases of thunderclouds over New Mexico, *Quart. J. Roy. Met. Soc.* **100**, 450-468 (1974).

47. Sukhorukov, J. R., Mishin, E. V., Stubbe, P. & Rycroft, M. J. On blue jet dynamics. *Geophys. Res. Letts.* **23**, 1625-1628 (1996).

48. Tong, L., Nanbu, K. & Fukunishi, H. Randomly stepped model for upward electrical discharge from top of thundercloud. *J. Phys. Soc. Japan* **74**, 1093-1095 (2005).

49. Goodman, S. J. & MacGorman, D. R. Cloud-to-ground lightning activity in mesoscale convective complexes. *Mon. Weath. Rev.* **114**, 2320-2328 (1986).

50. Brown, R. A., Kaufman, C. A., & MacGorman, D. R. Cloud-to-ground lightning associated with the evolution of a multicell storm. *J. Geophys. Res.* **107**, 4397 (2002).

51. Weins, K. C., Rutledge, S. A. & Tessendorf, S. A. The 29 June 2000 supercell observed during STEPS. Part II: Lightning and charge structure. *J. Atmos. Sci.* **62**, 4151-4177 (2005).

52. Mansell, E. R., MacGorman, D. R., Ziegler, C. L., Straka, J. M. Charge structure and lightning sensitivity in a simulated multicell thunderstorm. *J. Geophys. Res.* **110**, D12101 (2005).

53. Wescott, E. M. *et al.* Blue starters: Brief upward discharges from an intense Arkansas thunderstorm. *Geophys. Res. Letts.* **23**, 2153-2156 (1996).

54. Lang, T. J. & Rutledge, S. A. Kinematic, microphysical, and electrical aspects of an asymmetric bow-echo mesoscale convective system observed during STEPS 2000. *J. Geophys. Res.* in press, (2008).

55. van der Velde, O. *et al.* Analysis of the first gigantic jet recorded over continental North America. *J. Geophys. Res.* **112**, D20104 (2007).

56. MacGorman, D. R. *et al.* TELEX: The Thunderstorm Electrification and Lightning Experiment. *Bull. Amer. Meteorol. Soc.* in press, (2008).